JCTC Journal of Chemical Theory and Computation

Article

pubs.acs.org/JCTC

On Extension of the Current Biomolecular Empirical Force Field for the Description of Halogen Bonds

Michal Kolář[†,‡] and Pavel Hobza*[,†,§,∥]

[†]Institute of Organic Chemistry and Biochemistry and Gilead Science Research Center, Academy of Sciences of the Czech Republic, Flemingovo nam. 2, 166 10 Prague 6, The Czech Republic

[‡]Department of Physical and Macromolecular Chemistry, Faculty of Science, Charles University in Prague, Albertov 6, 128 43 Prague 2, The Czech Republic

[§]Regional Center of Advanced Technologies and Materials, Department of Physical Chemistry, Palacký University, Olomouc, 771 46 Olomouc, The Czech Republic

[∥]Department of Chemistry, Pohang University of Science and Technology, San 31, Hyojadong, Namgu, Pohang 790-784, Republic of Korea

Supporting Information

ABSTRACT: Until recently, the description of halogen bonding by standard molecular mechanics has been poor, owing to the lack of the so-called σ hole localized at the halogen. This region of positive electrostatic potential located on top of a halogen atom explains the counterintuitive attraction of halogenated compounds interacting with Lewis bases. In molecular mechanics, the σ hole is modeled by a massless point charge attached to the halogen atom and referred to as an explicit σ hole (ESH). Here, we introduce and compare three methods of ESH construction, which differ in the complexity of the input needed. The molecular mechanical dissociation curves of three model complexes containing bromine are compared with accurate CCSD(T)/CBS data. Furthermore, the performance of the Amber force field enhanced by the ESH on geometry characteristics is tested on the casein kinase 2 protein complex with seven brominated inhibitors. It is shown how various schemes depend on the selection of the ESH parameters and to what extent the energies and geometries are reliable. The charge of 0.2*e* placed 1.5 Å from the bromine atomic center is suggested as a universal model for the ESH.

1. INTRODUCTION

The halogen bond, a type of noncovalent interaction between a halogen atom and a Lewis base, has already been extensively studied and reviewed.[1−3] Despite the fact that halogens have higher electronegativity than carbon, which creates a negative partial charge on halogens in organic molecules, halogens favorably interact with a Lewis base atom, such as oxygen or nitrogen with a lone electron pair. This counterintuitive attraction is commonly explained by the existence of a region of positive electrostatic potential (ESP), located on top of the halogen atom.[4] This region, usually referred to as the σ hole, is an inherent feature of compounds containing covalently bound halogens; i.e., it is not induced by the interacting partner in a complex.

The halogen bond motif has been found in various crystalline materials as well as in biomolecular complexes and thus attracts the attention of current science.[5,6] It plays an especially important role in the design of novel drugs, and as many as about 40% of newly introduced drugs contain halogens.[7] It is believed that halogen bonding is at least partially responsible for the high biological action of these drugs. The basic problem which has triggered our interest in this field is that molecular mechanics (MM), which is almost exclusively used in *in silico* drug design, fails to describe halogen bonding (see below). The strength of the halogen bond reaches several kilocalories per mole and increases with the atomic number of the halogen—it is rather weak for chlorine and strongest for iodine. A fluorine atom covalently bound in organic molecules usually does not contain a σ hole, which turns into an inability to create a halogen bond in such systems.[3] When, however, fluorine is bound to a more electronegative atom than carbon, for instance to another fluorine, the σ hole is again formed.[8] Also, inorganic halogen-bonded complexes containing fluorine covalently bound to carbon were recognized.[9] Besides the electrostatic component of the interaction energy, dispersion was also shown to be essential, mainly owing to the close contacts of two atoms with high polarizability (C or N and halogen).[10]

Until recently, the description of halogen bonds with common biomolecular empirical force fields (e.g., the Amber family of force fields)[11,12] has been poor. Our observation of the faulty behavior of the General Amber Force Field (GAFF)[12] in the description of the protein−ligand interaction is certainly not rare.[13] Generally, the nonbonded interaction between a halogen atom and any other atom (as between any two atoms) within the empirical force field is characterized by a partial charge centered on the halogen and two Lennard-Jones (LJ) parameters standing effectively for Pauli repulsion and dispersion attraction. The polarization effects are either included implicitly in the prepolarized charge and LJ parameters[14,15] or explicitly via an additional polarizability

Received: November 22, 2011
Published: March 10, 2012

   dx.doi.org/10.1021/ct2008389 | J. Chem. Theory Comput. 2012, 8, 1325−1333

parameter. The anisotropy of the ESP around the halogen atom (i.e., σ hole), which is of quantum origin, is missing completely.

Very recently, a novel approach was suggested by Ibrahim,[16] who modeled a σ hole explicitly as a massless point charge placed on top of the halogen atom. He applied the explicit σ hole (called "extra point" in ref 16) to calculate the interaction energies and solvation energies as well as to run a short molecular dynamics of a protein−ligand complex. The procedure will be described and discussed below. In the past, the idea of an extra point charge (negative) in the force field was utilized to mimic a lone pair of Lewis bases.[17,18] While the use with halogens appears to be promising, a deeper insight into the construction of the σ hole as well as a revision of the comparison with the benchmark data seem to be needed.

The aim of this study is to provide several schemes of the explicit σ hole (ESH) construction and to compare the ability of the Amber empirical force field with and without the ESH to describe the energetics and geometrical features of halogen bonding. Recently,[19] we applied one of the schemes for an advanced scoring study of aldose reductase inhibitors, one of which contains halogen, with compelling results. Here, we have limited the complexes studied to the brominated ones, and besides the model systems we have also investigated protein−ligand complexes. It should be mentioned that the halogen bond in these systems contributes significantly to their biological action. The treatment of brominated compounds is the least problematic among halogens. The strength of the bromine halogen bond is significantly higher as compared to chlorine,[3,4] and the results are less biased by the eventual relativistic effects than they might be in the iodine case.

2. METHODS

2.1. ESH Construction. We studied three different ways to include the anisotropy of the ESP around the bromine atom described by the GAFF. Because of the electrostatic character of the σ hole, we have not applied any changes to the LJ parameters. We admit that a further reparameterization of LJ parameters might improve the results, but the design of the new halogen parameters does not seem to be as conspicuous as in the case of the σ hole.

In the first scheme, we calculated the molecular mechanical charges by means of the RESP methodology[20] and substituted the bromine point charge placed on the atomic center with two charges—the first representing a σ hole placed at a fixed distance from the bromine atomic center and the second representing a bromine atom. The σ-hole charge and bromine charge were chosen in such a way that the sum of them was equal to the bromine value obtained by the usual RESP fit. In other words, we subtract the ESH charge from the bromine charge. All of the other atomic partial charges were kept intact. In fact, we replaced the point charge of the bromine with a dipole moment, the size of which is parametrically dependent. The first approach, abbreviated here "nF" (as "no fit"), contains two parameters—the charge of the ESH and its distance from the atomic center of bromine. It should be noted that the atomic partial charges of all of the atoms have to be known prior to the construction of the σ hole. On the other hand, no further *ab initio* calculation is needed, which saves computational time significantly.

Contrary to the first approach, where no charges were modified during the construction of the ESH except for the charge of bromine, in the second scheme we chose the charge of the ESH and its distance and adjusted the partial charges of the rest of the molecule employing the RESP methodology. Two parameters had to be attributed to the ESH (i.e., charge and distance) in this approach, called "rF" (abbreviated as "rest fit"). The effect of the ESH is more delocalized across the molecule, and no charges need to be known prior to the construction of the ESH. More likely, the *ab initio* electrostatic potential grid has to be known in order to perform the RESP fit.

The third approach, abbreviated as "aF" ("all fit"), is identical to that introduced by Ibrahim. Fundamentally, only one parameter of ESH is needed here, i.e., the distance of the ESH from the bromine atomic center. The charge of the ESH was calculated by means of RESP. In other words, before the calculation of the partial charges using RESP, an additional fitting position was placed on top of the bromine atom. Undoubtedly, the charge of the ESH was as physically correct as possible (within the validity of the RESP technique) in this case. In ref 16, the ESH was allowed to move on the sphere of bromine providing the bond and angle force constants of Br−ESH and C−Br−ESH, respectively. We rather kept the position of the ESH fixed in order to be consistent with the previous two approaches and to reduce the number of degrees of freedom in the parametrization. Indeed, the origin and significance of the force constants in ref 16 comes from the previous studies of oxygen lone pairs.[17,18] We claim that the ESH should be constructed within the bromime van der Waals diameter. In the case of GAFF, the repulsion LJ parameter σ (not to be confused with the σ hole) is 1.8 Å (giving the r_{min} = 2.02 Å).[12] Since in the original paper, the ESH was placed out of this region, a repulsion LJ parameter was necessary to maintain the numerical stability of the calculation/simulation. We applied the σ LJ parameter of 1.00 Å as provided in ref 16.

The approaches are summarized in Table 1. The complexity of the input data differs across the schemes. While the nF scheme needs partial charges of the atoms (low complexity data), the rF and aF schemes require the *ab initio* grid of the electrostatic potential (highly complex data). Thus, the ratio of the accuracy/computer demands has to be considered as well.

Table 1. A Summary of the ESH Construction Schemes

parameters		nF (no fit)	rF (rest fit)	aF (all fit)
		charge, distance	charge, distance	distance
range	charge	0.05−0.50*e*	0.05 − 0.50*e*	
	distance	0.8−1.6 Å	0.8−1.6 Å	0.8−2.6 Å[a]
step	charge	0.05*e*	0.05*e*	
	distance	0.1 Å	0.1 Å	0.2 Å
charges needed a priori		yes	no	no
ab initio ESP grid needed		no	yes	yes

[a]The Br−ESH distance range was higher in the aF case to make the results comparable with the results from ref 15.

2.2. Gas-Phase Interaction Energies. To clarify the importance of particular ESH parameters, we compared the *ab initio* gas-phase dissociation curves calculated on the CCSD(T)/CBS level with the MM dissociation curves calculated with and without the ESH. As a reference method, we used the CCSD(T)/CBS technique, which, as the only QM method, describes the various motives of noncovalent interactions, including halogen bonding, with chemical (about 1 kcal/mol) or even subchemical (about 0.1 kcal/mol) accuracy.[21]

Table 2. The Location of the Energy Minima of the Dissociation Curves[a]

complex		Br2F_O	Br_O	Br_N
CCSD(T)/CBS	E_{min} [kcal/mol]	−2.43	−2.96	−3.62
	d_{min} [Å]	3.1	3.1	2.9
no ESH	E_{min} [kcal/mol]	−0.70	−0.38	−0.73
	d_{min} [Å]	3.5	3.5	3.5
nF	E_{min} [kcal/mol]	−3.14 (1.6, 0.10)	−2.28 (1.5, 0.10)	−3.83 (1.6, 0.20)
	d_{min} [Å]	3.1 (1.6, 0.10)	3.3 (1.5, 0.10)	3.3 (1.6, 0.20)
rF	E_{min} [kcal/mol]	−2.80 (1.5, 0.15)	−2.33 (1.5, 0.15)	−3.93(1.6, 0.30)
	d_{min} [Å]	3.1 (1.5, 0.15)	3.3(1.5, 0.15)	3.3 (1.6, 0.30)
aF	E_{min} [kcal/mol]	−2.90 (2.2)	−2.48 (2.0)	−2.18 (2.4)
	d_{min} [Å]	3.1 (2.2)	3.1 (2.0)	3.3 (2.4)

[a]Scheme without ESH (abbrev. "no ESH") as well as with ESH are shown for B3LYP charge sets. Where relevant, the ESH parameters are provided in the parentheses. MM values of E_{min} and d_{min} correspond to the lowest mean unsigned absolute error shown in Table 5.

Generally, the reference CCSD(T)/CBS data are accurate and adequately describe the dispersion interaction, unlike the DFT/B3LYP treatment or basis-set-superposition-error (BSSE) uncorrected MP2 treatment used in ref 16 as the benchmark. Since the dispersion energy contributes significantly[10] and sometimes dominantly to the halogen-bond stabilization, its nonadequate treatment can strongly affect the parametrization and/or verification of the ESH. Moreover, Lu and co-workers showed on the set of halogen bonded complexes that B3LYP performs rather poorly when compared with other DFT functionals.[22] The B3LYP average absolute error in interaction energy was as much as 0.86 kcal/mol, which was tens percent of the total interaction energies.[22]

In this study, the complete basis set values were estimated by the extrapolation of the aug-cc-pVDZ and aug-cc-pVTZ BSSE corrected values. The BSSE correction was done employing the counterpoise scheme of Boys and Bernardi.[23] For the CCSD(T) calculation, the Molpro program suite was used.[24] The studied complexes were bromobenzene···acetone (Br_O), bromobenzene···trimethylammonia (Br_N), and 1-bromo-3,5-difluorobenzene···acetone (Br2F_O).

The structures were prepared as follows: We started with an idealized halogen bond of the Br_O complex (C−Br···O angle = 180°, Br···O═C angle = 120°) and performed the full gradient optimization at the MP2/cc-pVTZ level. The final C−Br···O angle was 178.9°, but the same procedure in the Br2F_O case led to a structure significantly distorted by secondary (nonhalogen bonding) interactions. Since our major interest was in the halogen bond itself rather than in the overall interaction between the two molecules, we decided to keep the nearly ideal halogen bond distance and C−Br···O angle of the Br_O complex fixed for the Br2F_O case and optimize the rest. The Br_N complex was fully optimized at the MP2/cc-pVTZ level starting from the 180° C−Br···N angle. From the optimized structures, we generated a series of dissociative geometries by varying the intermolecular distance, while keeping all other geometrical parameters fixed. These geometries, which were not reoptimized, were used for CCSD(T) calculations of dissociation curves. Hence, these curves do not represent the true molecular separation from the minimum but rather a genuine halogen bond dissociation.

The geometric and energetic features of the complexes are summarized in Table 2. The structures with intermolecular distances corresponding to the lowest energy are shown in Figure 1. All of the geometries are available in xyz file format as the Supporting Information. The CCSD(T)/CBS interaction energies are shown in Table S1.

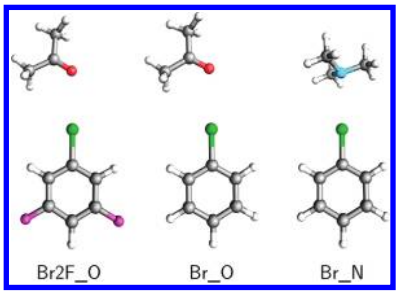

Figure 1. The structures of the complexes investigated in the gas phase. Br2F_O stands for the 1-bromo-3,5-difluorobenzene···acetone complex. Br_O stands for the bromobenzene···acetone complex, and Br_N stands for the bromobenzene···trimethylammonia complex.

For MM calculations, the monomers were optimized at the B3LYP/cc-pVTZ level followed by the calculation of the ESP grid points around the molecule. The grid was constructed with eight layers with a density of three points per unit area (see the Gaussian manual).[25] This option increases the statistical accuracy of the RESP procedure especially in the area around bromine, and as shown below it has a dramatic impact on the quality of the partial charges. The comparison of the MM and CCSD(T) gas-phase energies is not straightforward and might be questioned.[26−28] The reason is that the common biomolecular force fields were originally designed for the condensed phase. For instance, the charges obtained by the RESP fit onto the ESP grid points calculated at the HF/6-31G* level are usually higher in magnitude by about 15% than the real vacuum charges, which should, as proposed by Cornell et al.,[15] intentionally compensate for the missing polarization in the empirical force field.

Recently, a study about the polarization of σ holes was published.[29] On the set of hydrogen bonded complexes, the authors showed that polarization effects might have substantial effect on the extent of the σ hole. We assume that the extent of missing polarization in the force field is of similar magnitude as in the case of σ holes. Thus, to be consistent, the ESP grid points here were calculated at the HF/6-31G* level, as suggested by the developers of the General Amber Force Field, and also at the B3LYP/cc-pVTZ level. Using the DFT method with a significantly larger basis set provides vacuum charges which are not prepolarized and suitably represent the gas-phase electrostatics.[28] For each complex and each ESH variant, two charge sets were thus prepared.

It should be stressed that the MM gas phase calculations were performed to help build up an idea of how the energetics

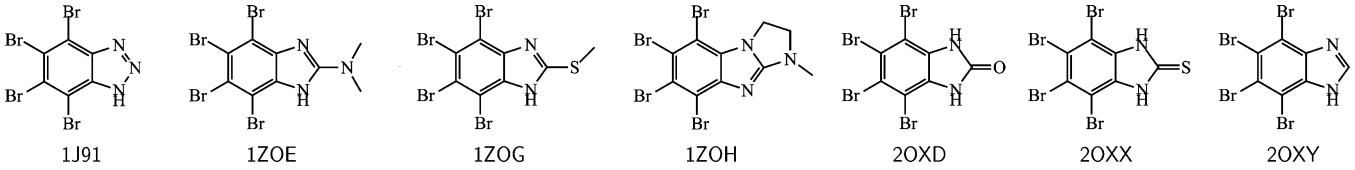

Figure 2. The structures of the tetrabrominated CK2 inhibitors and the corresponding PDB codes.

of halogen bonding is affected by various ESH parameters, while using liquid-phase parameters (i.e., LJ and bonding). Thus, for instance, we abandoned performing gas phase geometry optimizations, which would be difficult to interpret, indeed. Instead, we investigated the role of ESH on molecular geometries in the protein–ligand case (see bellow).

We performed a two-dimensional scan of the parameters in the nF and rF approaches and a one-dimensional scan for the aF approach. For each point (q, d) (charge, distance) or (d) (distance), we calculated the dissociation curve of all of the complexes. The calculations of the MM interaction energies were performed without cutoffs. The Gromacs program suite[29] was used for the MM calculations. The ESH was represented by a so-called virtual site algorithm available in the program as described by Berendsen and van Gunsteren.[31,32] This algorithm keeps the ESH position fixed with respect to the real atoms and redistributes the forces acting on ESH properly.

2.3. Optimization of Protein–Ligand Complexes. The effect of the ESH parameters on the geometry of a protein–ligand complex was tested on the set of casein kinase 2 (CK2) complexes, which we investigated recently.[13] The protein is inhibited by polyhalogenated ligands,[33−35] from which seven tetrabrominated ones were chosen. Their structural formulas are shown in Figure 2. High-quality X-ray structures are available in the Protein Data Bank under the codes 1J91, 1ZOE, 1ZOG, 1ZOH, 2OXD, 2OXX, and 2OXY.[36−38] All of the complexes were energy minimized, and the position of the ligand in the active site was evaluated.

The protein was described using the Amber parm03 force field[11,39] and the ligands using GAFF.[12] We used HF charge sets consistently with the force-field definitions. All of the bromines were enhanced by the ESH using all of the approaches mentioned (i.e., nF, rF, and aF). Such a system was energy minimized in the implicit Generalized Born model until the maximum force was lower than 2.4×10^{-5} kcal/mol/Å. The L-BFGS algorithm together with no cutoffs for interatomic interactions were used. To decrease the complexity of the problem, all of the heavy atoms except for the active site were under the position restraints of 12 kcal/mol/Å^2. The active site was chosen on the basis of visual inspection[40] and is shown in Figure 3. The same setup was used for minimizations without the ESH.

The root-mean-square deviation (RMSD) of the heavy atoms was calculated with respect to the X-ray structure. At first, the backbone coordinates of the minimized structure were aligned onto the X-ray coordinates, followed by the separate calculations of ligand and active-site amino acid RMSDs. The number of oxygen atoms within a 3.5 Å vicinity of the bromine atoms was calculated. The value stands for the approximate number of the halogen bonds between the ligand and protein. This was done for all of the ESH parameters summarized in Table 1.

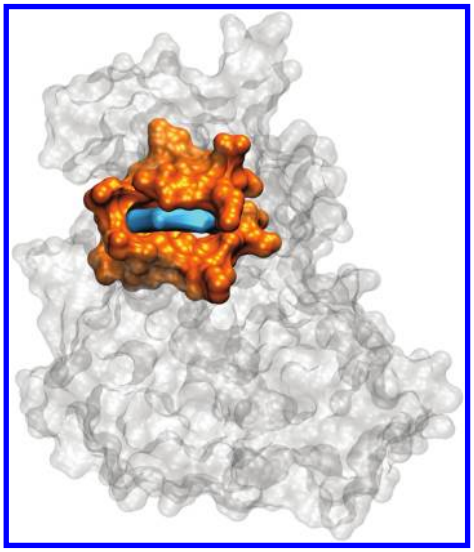

Figure 3. The overall shape of the CK2 protein. The selection of the active-site amino acids (orange) and the ligand (blue) were allowed to move freely during the optimization. The remaining amino acids (gray) were subject to position restraints of 12 kcal/mol/Å^2.

3. RESULTS AND DISCUSSION

3.1. Gas-Phase Interaction Energies. The introduction of the ESH led to the variation of the bromine and other atomic partial charges. The representative values of the charges are shown in Table 3. The aF charges are considered to be more physically sound than those of the nF and rF. The charges of the ESH and the closest atoms vary with the Br–ESH distance, and these variations are similarly pronounced for the rF and aF schemes. In contrast, the nF scheme by definition varies the ESH and Br charges differently, and the other charges are kept intact (see Methods). When the aF ESH charges in bromobenzene and 1-bromo-3,5-difluorobenzene are compared, the latter contains a less positively charged ESH. However, the magnitude of the σ hole should be higher in fluorinated bromobenzene, as discussed in ref 41. The lower ESH charge in the case of 1-bromo-3,5-difluorobenzene is thus quite counterintuitive. It seems that the counterintuitive ESH charges are a consequence of the RESP fitting scheme we used, where we did not employ the default Gaussian program setup for ESP grid calculation (4 layers, density 1 point/Å) but enhanced ESP grid (8 layers, density 3 points/Å). Interestingly, we found that when the default ESP grid is used for RESP fitting, the resulting ESH charges are intuitive (i.e., ESH is more positive for 1-bromo-3,5-difluorobenzene compared with bromobenzene). We investigated a set of halogenated molecules[42] with different ESP grids. We conclude that for denser ESP grids, we obtained a better RESP fit in terms of relative ESP root-mean-square error (not shown), although the dipole moments were not always improved. The unlikely performance of RESP fitting procedure might be attributed to the complicated ESP shape around the halogen atom.

Table 3. The B3LYP Atomic Partial Charges of the Bromobenzene and 1-Bromo-3,5-Difluorobenzene Calculated Using Various Schemes[a]

	bromobenzene				
	d/Å	no ESH	nF	rF	aF
ESH	0.8		0.30	0.30	0.29447
	1.2		0.15	0.15	0.15965
	1.6		0.10	0.10	0.09641
Br	0.8	−0.07145	−0.37145	−0.58701	−0.57727
	1.2	−0.07145	−0.22145	−0.38922	−0.41041
	1.6	−0.07145	−0.17145	−0.32663	−0.31709
C	0.8	−0.13085	−0.13085	0.31959	0.30966
	1.2	−0.13085	−0.13085	0.23242	0.26086
	1.6	−0.13085	−0.13085	0.22171	0.20644
	1-bromo-3,5-difluorobenzene				
	d/Å	no ESH	nF	rF	aF
ESH	0.8		0.20	0.20	0.20462
	1.2		0.10	0.10	0.11694
	1.6		0.10	0.10	0.07350
Br	0.8	−0.0802	−0.21802	−0.36148	−0.36957
	1.2	−0.0802	−0.11802	−0.23042	−0.26715
	1.6	−0.0802	−0.11802	−0.27764	−0.20684
C	0.8	−0.17183	−0.17183	0.13140	0.13948
	1.2	−0.17183	−0.17183	0.07823	0.12575
	1.6	−0.17183	−0.17183	0.21757	0.10058

[a]Only the ESH, bromine and carbon covalently bound to bromine are shown. The values for several Br-ESH distances *d* are shown. Note that in the nF and rF cases, the ESH charge is an arbitrary parameter while in the aF case it is calculated from the *ab initio* data. The charges from the unmodified force field are provided in "no ESH" column. For details about the schemes, see the Methods section.

In Figure 4, the ESP of the σ hole calculated at the B3LYP/cc-pVTZ and various MM schemes is shown. Qualitatively wrong results of the model lacking ESH are apparent (second row plots). No region with positive ESH results from the original force field in contrast with ESH schemes. Indeed, the electrostatic potentials of the benzenes are well behaved in all of the ESH schemes, and Br2F experiences a region which is more positively charged, in agreement with the *ab initio* data.[41] The MM electrostatic potential plots were calculated with the charges derived from the denser ESH grid (i.e., 8 layers, 3 points/Å) calculated at B3LYP/cc-pVTZ. This is, no doubt, an important finding, showing that the simple MM treatment enhanced by ESH is able to describe effectively a complicated induction and the polarization effects of fluorines on bromine.

Table 4 shows the dipole moments for various ESH models and relative root-mean-square errors (RRMS) of the MM ESP with respect to the QM ESP. Standard RESP fit without any ESH yields quite good dipole moments differing by less that 0.2 D. When ESH was introduced by the simplest nF scheme, the dipole moments worsened notably, differing by about 0.4 D. Both "fitting" schemes (i.e., rF and aF) perform much better, providing better dipole moments than the scheme without ESH. The quality of the RESP fit in terms of RRMS is also improved when ESH is included by rF or aF schemes. The simplest nF scheme is not based on ESP generation, hence no RRMS values are provided.

The magnitude of the charges has a direct effect on the dissociation curves. The representative dissociation curves are plotted in Figure 5. For all of the dissociation curves, we have calculated the mean unsigned absolute error (MUAE) and

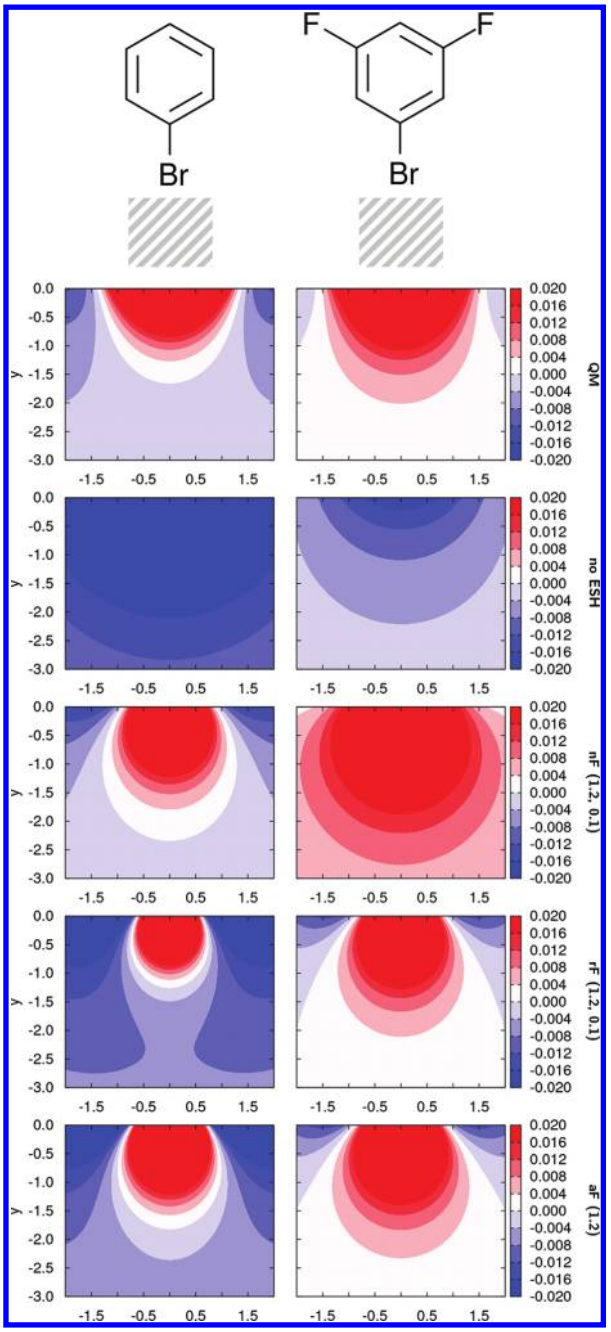

Figure 4. The electrostatic potential maps of the σ hole for bromobenzene (left) and 1-bromo-3,5-difluorobenzene (right). The negative values are in blue, the positive in white and red. The ESP in the hatched areas was calculated at the B3LYP/cc-pVTZ level (abbrev. QM), with the standard MM (abbrev. "no ESH") and with three ESH schemes. The ESH is located at $x = 0.0$, $y = 0.0$. The bromine atom is located at $x = 0.0$, $y = 1.2$. The charge parameter of the nF and rF schemes was chosen to be 0.10*e*.

mean unsigned relative error (MURE) according to eqs 1 and 2.

$$\mathrm{MUAE} = \frac{1}{N}\sum_i^N |E_i(\mathrm{MM}) - E_i(\mathrm{QM})| \quad (1)$$

$$\mathrm{MURE} = \frac{1}{N}\sum_i^N \left|\frac{E_i(\mathrm{MM}) - E_i(\mathrm{QM})}{E_i(\mathrm{QM})}\right| \quad (2)$$

dx.doi.org/10.1021/ct2008389 | J. Chem. Theory Comput. 2012, 8, 1325−1333

Table 4. RESP Fit Characteristics[a]

molecule	bromobenzene	1-bromo-3,5-difluorobenzene
μ [D] (QM)	1.83	0.11
μ [D] (no ESH)	1.99	0.16
μ [D] (nF: 1.2, 0.1)	1.42	0.40
μ [D] (rF: 1.2, 0.1)	1.95	0.13
μ [D] (aF: 1.2)	1.93	0.12
RRMS [%] (no ESH)	18.8	23.0
RRMS [%] (nF: 1.2, 0.1))		
RRMS [%] (rF: 1.2, 0.1)	12.5	14.5
RRMS [%] (aF: 1.2)	10.6	13.9

[a]Dipole moments for various ESH models and relative root mean square errors (RRMS) of the MM ESP with respect to the QM ESP. Only results for B3LYP charge set are shown.

where N is the number of points of the dissociation curves and E(MM) and E(QM) are the interaction energies calculated with a force field or on an *ab initio* level, respectively. Both quantities express how well the dissociation curves are represented with respect to the references data. While the MUAE presented in kilocalories per mole shows the absolute difference between the curves, the MURE presented in percentage (%) describes the relative difference. No information about the overestimation or underestimation of the interaction energies is provided. Owing to the enormous errors of the repulsion parts of the curves (not shown), only the points which are farther than the minima of the CCSD(T)/CBS curves were considered. For the B3LYP charge sets, the lowest MUAE and MURE are summarized in Tables 5 and 6. The plots MUAE and MURE as well as the dissociation curves for all of the ESH parameters are provided as Supporting Information.

The B3LYP charge sets are discussed first and the HF charge sets are mentioned below. First, a complete failure of the unmodified force field is apparent. The MUAE reaches about 1 kcal/mol for complexes of acetone and almost 3 kcal/mol for a complex of trimethylammonia, which is comparable with the absolute values of the interaction energies. This fact is well reflected by the high values of the MURE, reaching as much as 300% in the bromobenzene···acetone case. The inclusion of the ESH by any scheme improves the results greatly. The improvement of the acetone complex results is more pronounced than that of trimethylammonia. We claim that this is probably because of the higher electrostatic nature of the interaction in the acetone cases. The electrostatic contribution, originally not covered by the force field well, is corrected for by

Table 5. The Lowest Mean Unsigned Absolute Error (MUAE) for $R > R_{eq}$[a]

	B3LYP			
	no ESH	nF	rF	aF
Br2F_O	1.17	0.17 (1.6, 0.10)	0.09 (1.5, 0.15)	0.05 (2.2)
Br_O	1.16	0.14 (1.5, 0.10)	0.08 (1.5, 0.15)	0.04 (2.0)
Br_N	2.93	0.83 (1.6, 0.20)	0.73 (1.6, 0.30)	1.27 (2.4)
	HF			
	no ESH	nF	rF	aF
Br2F_O	1.18	0.16 (1.4, 0.10)	0.09 (1.4, 0.15)	0.03 (2.0)
Br_O	1.29	0.13 (1.5, 0.10)	0.06 (1.3, 0.20)	0.10 (2.0)
Br_N	3.13	0.84 (1.6, 0.15)	0.72 (1.6, 0.25)	0.98 (2.4)

[a]The ESH parameters (d, q) for the nF and rF schemes or (d) for the aF scheme are provided in parentheses. The results of the unmodified force field not containing the ESH are shown in the "no ESH" column. The MUAE values are in kcal/mol, the distance in Å, and the charge in e.

Table 6. The Lowest Mean Unsigned Relative Error (MURE) for $R > R_{eq}$[a]

	B3LYP			
	no ESH	nF	rF	aF
Br2F_O	75.1	20.0 (1.6, 0.05)	6.2 (1.4, 0.15)	8.6 (2.2)
Br_O	306.2	31.2 (1.6, 0.05)	13.0 (1.0, 0.30)	42.5 (2.0)
Br_N	106.4	57.5 (1.6, 0.10)	41.9 (1.6, 0.20)	38.0 (2.4)
	HF			
	no ESH	nF	rF	aF
Br2F_O	75.6	19.0 (1.6, 0.05)	4.1 (1.6, 0.10)	4.0 (2.0)
Br_O	417.0	28.1 (1.2, 0.10)	19.1 (0.9, 0.45)	122.2 (2.0)
Br_N	122.2	51.7 (1.6, 0.10)	35.8 (1.6, 0.20)	32.6 (2.4)

[a]The ESH parameters (d, q) for the nF and rF schemes or (d) for the aF scheme are provided in parentheses. The results of the unmodified force field not containing the ESH are shown in the "no ESH" column. The MURE values are in %, the distance in Å, and the charge in e.

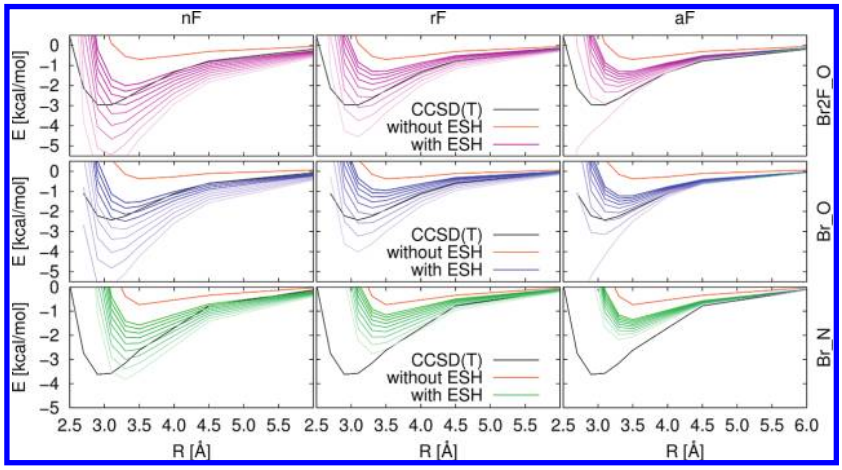

Figure 5. The dependence of the dissociation curves on the Br-ESH distance. The results for a charge of 0.20e in the nF and rF cases are shown. The charge of the aF is calculated exactly (see Methods). The lighter the curve is, the larger the Br−ESH distance used. The dissociation curve calculated with the force field lacking the ESH is plotted in orange; the reference *ab initio* data are in black.

dx.doi.org/10.1021/ct2008389 | J. Chem. Theory Comput. 2012, 8, 1325−1333

the ESH. Other drawbacks of the force field, such as the unreliable repulsion part, which is largely pronounced in the Br_N case, are not directly connected with the ESH concept and hence cannot really be corrected for by ESH.

Both rF and aF perform better than nF. It should not be surprising, because the atomic charge set in the rF and aF schemes represents the true *ab initio* electrostatic potential better than nF. The nF electrostatic potential is slightly overestimated as shown in Figure 4, third row, as compared with rF and aF (Figure 4, fourth and fifth rows) for both halogenated benzenes. The MUAE of the acetone complexes for the rF and aF schemes is lower than 0.1 kcal/mol and slightly higher (about 0.15 kcal/mol) for the nF scheme. For the trimethylammonia case, the two-parameter models (nF and rF) perform better than one-parameter models (aF), providing MUAEs of 0.83, 0.73, and 1.27, respectively, still much better than the original force field without the ESH. In this context, it should be noted that the additional degree of freedom, i.e., the charge, in the nF and rF cases, unlike with aF, might compensate for the worse repulsion in the Br_N case, yielding better results for nF and rF than aF.

Generally, for two parameter models, the lowest MUAE and MURE were obtained with rather higher Br−ESH distances (above 1.4 Å) and lower ESH charges (below 0.20*e*). However, the lowest MUAE of all was calculated by the one-parameter aF model. The Br−ESH distance of 2.0 Å in this case is questionable owing to the need for an ESH repulsion parameter.

Table 2 shows the optimum distances, absolute interaction energies, and ESH parameters for the curves with the lowest MUAE. The numbers suggest that the repulsion parameter of bromine should be addressed in the future since almost all of the lowest MUAE curves' minima lie in somewhat too high distances.

3.2. Different Charge Sets. The lowest MUAE and MURE for the HF charge sets are presented in Tables 5 and 6. Due to the larger magnitude of the charges as compared to B3LYP charges, the differences between the various *d* and *q* or *d* parameters were slightly more pronounced. The best MUAE and MURE values are fully comparable with the B3LYP charge sets, and the overall behavior of the parameter dependence is also similar, as shown in Figures S1, S2, and S3.

3.3. Optimization of Protein−Ligand Complexes. We investigated the effect of the *d* and *q* or *d* parameter selection on the quality of the optimized protein−ligand geometries. The representative root-mean-square deviations (RMSDs) of the ligand with respect to the X-ray structure are depicted in Figure 6 in red, and those of the entire active site are depicted in blue. Only the results for the 1ZOE complex are shown. The RMSD plots for all of the ligands are provided in Supporting Information, Figure S4. The projections of the 3D plots represent the nF and rF schemes (Figure 6, first and second rows); the 2D plot is for the aF approach (Figure 6, third row). In the 3D plots, the darker the color is and the higher the RMSD the optimized structure has, the worse the result it represents. Note the different ranges of the colors. In orange, the number of the protein oxygen atoms which are located closer than 3.5 Å to the ligand bromine atoms is shown (abbreviated as "xbs"). The numbers of "xbs" halogen−oxygen contacts for all of the ligands are provided in the Supporting Information, Figure S6.

Two-dimensional models (nF, rF) provide better results for higher Br−ESH distances and higher ESH charges (the bright areas in Figures 6 and S4). The closer contact of the ESH with protein oxygen atoms tends to stabilize the correct geometry of the protein−ligand complex. The RMSDs of the entire active site are noisier, but a trend similar to ligand RMSDs is apparent. Moreover, the range of the values is narrower as compared to the ligand values. It should be noted that despite the fact that in the nF and rF cases the charges of all four bromine atoms were chosen to be identical, the bromine atoms do not behave identically in the calculations. The vicinity of bromines creates a unique electrostatic potential around each of the bromine atoms, thus assuring the requirement of the distinguishability between them in accordance with chemical intuition.

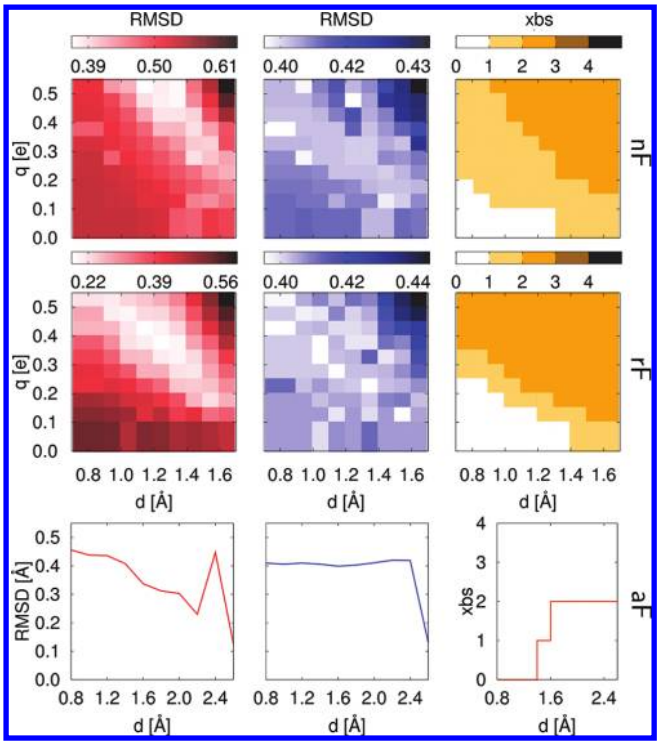

Figure 6. The optimization results of the 1ZOE complex. Two-dimensional scans of the *d* and *q* parameters were performed for the nF and rF schemes (the first and second row); a one-dimensional scan was conducted for the aF scheme (the third row). The RMSDs of the ligand with respect to the active side are depicted in red; the RMSDs of the entire active site are depicted in blue. The numbers of oxygen atoms "xbs" located within 3.5 Å of the bromine atoms are in orange. For comparison, the X-ray structure contains two bromine−oxygen contacts (i.e., xbs = 2), and the force field lacking the ESH provided a structure without any bromine−oxygen contact (i.e., xbs = 0).

The X-ray bromine−oxygen contacts vary between zero (1J91 complex) and three (1ZOH complex). As shown in Figure S6, the regions of the (*d*, *q*) space which provide the correct number of bromine−oxygen contacts are similar to those with lower ligand RMSDs (i.e., larger Br−ESH distance and higher charge). The results of the one-parameter aF scheme are fully comparable with two-parameter schemes.

The summary of the lowest ligand RMSDs is shown in Table 7. We defined a quality "success" as a percentage number of parameter combinations (*d*, *q*) which provided a lower RMSD than the unmodified force field without the ESH. For the aF approach, the quantity is defined in a similar one-dimensional manner. The higher the success is, the less parameter-dependent the scheme appears to be. The success values are provided also in Table 7.

dx.doi.org/10.1021/ct2008389 | J. Chem. Theory Comput. 2012, 8, 1325−1333

Table 7. The Lowest RMSDs of the Ligands with Respect to the X-Ray Structures[a]

PDB code	no ESH	nF [Å]	rF [Å]	aF [Å]
1J91	1.31	0.57 (90%)	0.34 (100%)	0.56 (100%)
1ZOE	0.45	0.37 (59%)	0.13 (92%)	0.12 (100%)
1ZOG	0.58	0.30 (100%)	0.33 (100%)	0.07 (100%)
1ZOH	0.48	0.49 (0%)	0.49 (0%)	0.26 (10%)
2OXD	0.72	0.37 (100%)	0.27 (71%)	0.03 (100%)
2OXX	0.60	0.23 (91%)	0.43 (96%)	0.06 (90%)
2OXY	1.94	0.22 (100%)	0.17 (96%)	0.06 (100%)

[a]The success values are provided in parentheses. For comparison, also the results of the unmodified force field are shown in the "no ESH" column.

The unmodified force field yielded the lowest ligand RMSD for the 1ZOH case (0.48 Å) but the highest RMSD for 2OXY (1.94 Å). Considering the size of the ligand, all of the values higher than 1.0 Å might be considered as a significant failure. The RMSDs for the nF case are quite similar or better than the unmodified force field, and a high percentage of ESH (d, q) combinations provides an improvement of the ligand geometry within the active site of the protein. An exception is the 1ZOH case, where no (d, q) combination led to a lower RMSD in both the nF and rF schemes. The reasons are 2-fold—first, the unmodified force field itself already provides quite good agreement with the X-ray data, and second, the higher RMSD is mostly caused by the undesirable movement of the five-member ring of the ligand upon minimization. However, the number of bromine−oxygen contacts in the 1ZOH case was indeed improved by adding the ESH into the force field (see Figure S6).

The rF results are very similar to those of nF. The 1ZOH problem is still pronounced, but the success values are slightly better than for the other ligands. Two-parameter schemes are thus quite comparable in spite of the different quality of the partial charges. The one-parameter aF scheme provided much lower RMSDs as compared to the unmodified force field. In four cases, values lower than 0.1 Å were obtained, which is certainly a remarkable result. However, like in the gas phase calculations, the best results were obtained for rather high Br−ESH distances (2.2 Å or more). When one keeps in mind that the common halogen-bond length (i.e., the distance between the halogen and Lewis base) is about 3.2 Å, then the position of the ESH in the best performing aF force-field modifications is only about 1 Å. This might be undesirable for force-field calculations as well as for MD because of the high probability of a collision of the respective atoms. The physical correctness of this charge alignment is still questionable. High success values across the schemes suggest that any force-field enhancement by the ESH is promising and needed.

4. SUMMARY

We have presented and compared three schemes for the description of the anisotropy of the charge distribution of halogenated ligands in molecular mechanics. The molecular mechanical explicit σ hole (ESH) was constructed as a massless point charge. The one-parameter model aF provided excellent results in both the gas-phase calculations and protein−ligand geometry optimization, but only for very high Br−ESH distances (more than 2.0 Å) beyond the bromine vdW radius. The charge of the ESH fitted to the electrostatic-potential grid seems to be somewhat too small to ensure significant improvement when placed within the bromine van der Waals radius. When placed further outside, the ESH performs much better, but probably for wrong reasons. The ESH then is very close (even less than 1 Å) to the electron-donor atom.

Both two-parameter models nF and rF performed slightly worse as compared to the aF scheme. The rF scheme gas-phase interaction energies were better than the nF owing to a more physical description of the electrostatic potentials of the halogenated molecules. The results of the protein−ligand geometry optimizations were very similar. Generally, all of the calculations with the ESH surpass those without ESH.

The practical aspects were considered with the following conclusions: Placing the ESH outside the van der Waals radius might cause numerical instabilities of MD simulations. Thus, a modest overestimation of the ESH charge makes it possible to reach sufficiently short Br−ESH distances. For the adjustment of the other atomic charges, an electrostatic-potential grid based on *ab initio* calculation is needed. This might be a complication for large molecules or for a high number of molecules studied (e.g., drug-design docking/scoring studies). In that case, the nF scheme is an acceptable alternative because the time-consuming ESP grid generation is not necessary.

We showed that ESP is well represented by a low charged ESH placed about 1.2 Å from the bromine mass center. Perhaps, due to the poor repulsion part of the force field, particularly bromine, the best results (in terms of energy as well as protein−ligand geometry) were obtained with ESH at a larger distance form the halogen. According to our results, we suggest a Br−ESH distance of 1.5 Å and an ESH charge of 0.20e as competent parameters for brominated molecules. Similar results might be expected when a higher charge is attached closer to the bromine atomic center, although with a better stability of the simulations. Indeed, these universal parameters might be improved by a careful parametrization targeted to the specific molecules/problems, but we believe that for the majority of the problems solved by molecular mechanics the parameters are sufficiently reliable.

To prove the ESH concept completely, an application to molecular dynamics is also needed. Certainly, it is beyond the scope of this paper, but quantities such as liquid densities or molecular hydration energies have to be addressed.

■ ASSOCIATED CONTENT

Supporting Information

The geometries of the complexes used for the dissociation-curve calculations, the CCSD(T)/CBS interaction energies, mean unsigned absolute errors (MUAE) and mean unsigned relative errors (MURE) for the B3LYP and HF charge sets, the root-mean-square deviations of the CK2 inhibitors and CK2 active sites, and the numbers of inhibitor bromines and protein oxygen atoms. This material is available free of charge via Internet at http://pubs.acs.org.

■ AUTHOR INFORMATION

Corresponding Author

*Tel.: (+420) 220 410311. E-mail: pavel.hobza@uochb.cas.cz.

Notes

The authors declare no competing financial interest.

■ ACKNOWLEDGMENTS

The authors are grateful to Dr. Kevin E. Riley for providing the reference dissociation curves and for valuable discussions and to

Dr. Tomáš Kubař for the discussions of the RESP fitting. This work was supported by the Institute of Organic Chemistry and Biochemistry, Academy of Sciences of the Czech Republic [Z40550506], the Czech Science Foundation [P208/12/G016], and Korea Science and Engineering Foundation [World Class Univ. program: R32-2008-000-10180-0]. This work was also supported by the Operational Program Research and Development for Innovations—European Science Fund (CZ.1.05/2.1.00/03.0058). The support of Praemium Academiae, Academy of Sciences of the Czech Republic, awarded to P.H. in 2007 is also acknowledged.

REFERENCES

(1) Lommerse, J. P. M; Stone, A. J.; Taylor, R.; Allen, F. H. *J. Am. Chem. Soc.* **1996**, *118*, 3108−3116.
(2) Auffinger, P.; Hays, F. A.; Westhof, E.; Ho, P. S. *Proc. Natl. Acad. Sci. USA* **2004**, *101*, 16789−16794.
(3) Politzer, P.; Lane, P.; Concha, M.; Ma, Y.; Murray, J. *J. Mol. Model.* **2007**, *13*, 305−311.
(4) Clark, T.; Hennemann, M.; Murray, J. S.; Politzer, P. *J. Mol. Model.* **2007**, *13*, 291−296.
(5) Metrangolo, P.; Neukirch, H.; Pilati, T.; Resnati, G. *Acc. Chem. Res.* **2005**, *38*, 386−395.
(6) Lu, Y.; Shi, T.; Wang, Y.; Yang, H.; Yan, X.; Luo, X.; Jiang, H.; Zhu, W. *J. Med. Chem.* **2009**, *52*, 2854−2862.
(7) Parisini, E.; Metrangolo, P.; Pilati, T.; Resnati, G.; Terraneo, G. *Chem. Soc. Rev.* **2011**, *40*, 2267−2278.
(8) Munusamy, E.; Sedlák, R.; Hobza, P. *ChemPhysChem* **2011**, *12*, 3253−3261.
(9) Lu, Y. X.; Zou, J. W.; Yu, Q. S.; Jiang, Y. J.; Zhao, W. N. *Chem. Phys. Lett.* **2007**, *449*, 6−10.
(10) Riley, K. E.; Hobza, P. *J. Chem. Theory Comput.* **2008**, *4*, 232−242.
(11) Duan, Y.; Wu, C.; Chowdhury, S.; Lee, M. C.; Xiong, G.; Zhang, W.; Yang, R.; Cieplak, P.; Luo, R.; Lee, T.; Caldwell, J.; Wang, J.; Kollman, P. *J. Comput. Chem.* **2003**, *24*, 1999−2012.
(12) Wang, J.; Wolf, R. M.; Caldwell, J. W.; Kollman, P. A.; Case, D. A. *J. Comput. Chem.* **2004**, *25*, 1157−1174.
(13) Dobeš., P.; Řezáč, J.; Fanfrlík, J.; Otyepka, M.; Hobza, P. *J. Phys. Chem. B* **2011**, *115*, 8581−8589.
(14) Jorgensen, W. L.; Tirado-Rives, J. *J. Am. Chem. Soc.* **1988**, *110*, 1657−1666.
(15) Cornell, W. D.; Cieplak, P.; Bayly, C. I.; Kollmann, P. A. *J. Am. Chem. Soc.* **1993**, *115*, 9620−9631.
(16) Ibrahim, M. A. A. *J. Comput. Chem.* **2011**, *32*, 2564−2574.
(17) Dixon, R. W.; Kollman, P. A. *J. Comput. Chem.* **1997**, *18*, 1632−1646.
(18) Cieplak, P.; Caldwell, J.; Kollman, P. *J. Comput. Chem.* **2001**, *22*, 1048−1057.
(19) Fanfrlík, J.; Kolář, M.; Lepšík, M; Musuramy, E.; Řezáč, J.; Hobza, P. In preparation.
(20) Bayly, C. I.; Cieplak, P.; Cornell, W.; Kollman, P. A. *J. Phys. Chem.* **1993**, *97*, 10269−10280.
(21) Riley, K. E.; Pitoňák, M.; Jurečka, P.; Hobza, P. *Chem. Rev.* **2010**, *110*, 5023−5063.
(22) Lu, Y. X.; Zou, J. W.; Fan, J. C.; Zhao, W. N.; Jiang, Y. J.; Yu, Q. S. *J. Comput. Chem.* **2009**, *30*, 725−732.
(23) Boys, S. F.; Bernardi, F. *Mol. Phys.* **1970**, *19*, 553−566.
(24) Werner, H. J.; Knowles, P. J.; Knizia, G.; Manby, F. R.; Schütz, M.; *MOLPRO*, version 2010.1; Cardiff University: Cardiff, Wales; Universität Stuttgart: Stuttgart, Germany, 2010.
(25) Frisch, M. J.; Trucks, G. W.; Schlegel, H. B.; Scuseria, G. E.; Robb, M. A.; Cheeseman, J. R.; Scalmani, G.; Barone, V.; Mennucci, B.; Petersson, G. A.; Nakatsuji, H.; Caricato, M.; Li, X.; Hratchian, H. P.; Izmaylov, A. F.; Bloino, J.; Zheng, G.; Sonnenberg, J. L.; Hada, M.; Ehara, M.; Toyota, K.; Fukuda, R.; Hasegawa, J.; Ishida, M.; Nakajima, T.; Honda, Y.; Kitao, O.; Nakai, H.; Vreven, T.; Montgomery, J. A., Jr.; Peralta, J. E.; Ogliaro, F.; Bearpark, M.; Heyd, J. J.; Brothers, E.; Kudin, K. N.; Staroverov, V. N.; Kobayashi, R.; Normand, J.; Raghavachari, K.; Rendell, A.; Burant, J. C.; Iyengar, S. S.; Tomasi, J.; Cossi, M.; Rega, N.; Millam, N. J.; Klene, M.; Knox, J. E.; Cross, J. B.; Bakken, V.; Adamo, C.; Jaramillo, J.; Gomperts, R.; Stratmann, R. E.; Yazyev, O.; Austin, A. J.; Cammi, R.; Pomelli, C.; Ochterski, J. W.; Martin, R. L.; Morokuma, K.; Zakrzewski, V. G.; Voth, G. A.; Salvador, P.; Dannenberg, J. J.; Dapprich, S.; Daniels, A. D.; Farkas, Ö.; Foresman, J. B.; Ortiz, J. V.; Cioslowski, J.; Fox, D. J. *Gaussian 09*, Revision A.1; Gaussian, Inc.: Wallingford, CT, 2009.
(26) Paton, R. S.; Goodman, J. M. *J. Chem. Inf. Model.* **2009**, *49*, 944−955.
(27) Kolář, M.; Berka, K.; Jurečka, P.; Hobza, P. *ChemPhysChem* **2010**, *11*, 2399−2408.
(28) Zgarbová, M.; Otyepka, M.; Šponer, J.; Hobza, P.; Jurečka, P. *Phys. Chem. Chem. Phys.* **2010**, *12*, 10476−10493.
(29) Hennemann, M.; Murray, J. S.; Politzer, P.; Riley, K. E.; Clark, T. *J. Mol. Model.* **2011**, DOI: 10.1007/s00894-011-1263-5.
(30) Hess, B.; Kutzner, C.; van der Spoel, D.; Lindahl, E. *J. Chem. Theory Comput.* **2008**, *4*, 435−447.
(31) Berendsen, H. J. C.; van Gunsteren, W. F. Molecular dynamics simulations: Techniques and approaches. In *Molecular Liquids-Dynamics and Interactions*; Barnej, A. J., Orville-Thomas, W. J., Yarwood, J., Eds.; D. Reidel: Dordrecht, The Netherlands, 1984; NATO ASI C 135, pp 475−500.
(32) van der Spoel, D.; Lindahl, E.; Hess, B.; van Buuren, A. R.; Apol, E.; Meulenhoff, P. J.; Tieleman, D. P.; Sijbers, A. L. T. M.; Feenstra, K. A.; van Drunen, R.; Berendsen, H. J. C. Interaction function and force field. *Gromacs User Manual*; version 4.5.4; University of Uppsala: Uppsala, Sweden, 2010.
(33) Pagano, M. A.; Bain, J.; Kazimierczuk, Z.; Sarno, S.; Ruzzene, M.; Di Maira, G.; Elliott, M.; Orzeszko, A.; Cozza, G.; Meggio, F.; Pinna, L. A. *Biochem. J.* **2008**, *415*, 353−365.
(34) Gianoncelli, A.; Cozza, G.; Orzeszko, A.; Meggio, F.; Kazimierczuk, Z.; Pinna, L. A. *Bioorg. Med. Chem.* **2009**, *17*, 7281−7289.
(35) Cozza, G.; Bortolato, A.; Moro, S. *Med. Res. Rev.* **2010**, *30*, 419−462.
(36) De Moliner, E.; Brown, N. R.; Johnson, L. N. *Eur. J. Biochem.* **2003**, *270*, 3174−3181.
(37) Battistutta, R.; Mazzorana, M.; Sarno, S.; Kazimierczuk, Z.; Zanotti, G.; Pinna, L. A. *Chem. Biol.* **2005**, *12*, 1211−1219.
(38) Battistutta, R.; Mazzorana, M.; Cendron, L.; Bortolato, A.; Sarno, S.; Kazimierczuk, Z.; Zanotti, G.; Moro, S.; Pinna, L. A. *ChemBioChem* **2007**, *8*, 1804−1809.
(39) Sorin, E.; Pande, V. S. *Biophys. J.* **2005**, *88*, 2472−2493.
(40) Contains the following amino acids: Val45, Gly46, Arg47, Ser51, Glu52, Val53, Ile66, Ile67, Lys68, Glu81, Val95, Lys96, Phe113, Glu114, Tyr115, Val116, Asn118, His160, Asn161, Met163, Arg172, Ile174, Asp175, and Gly177.
(41) Riley, K.; Murray, J.; Fanfrlík, J.; Řezáč, J.; Solá, R.; Concha, M.; Ramos, F.; Politzer, P. *J. Mol. Model.* **2011**, *17*, 3309−3318.
(42) Bromobenzene, chlorobenzene, 1-bromo-3,5-difluorobenzene, bromoethane, chloroethane, bromomethane, chloromethane, 3-bromo-pro-1-en, 3-chloro-prop-2-en, 4-bromotoluene, and 2-chlorotoluene.